Virologica Sinica 38 (2023) 84–95

Contents lists available at ScienceDirect

Virologica Sinica

journal homepage: www.keaipublishing.com/en/journals/virologica-sinica
www.virosin.org

Research Article

Identification of African swine fever virus MGF505-2R as a potent inhibitor of innate immunity *in vitro*

Huaguo Huang [a,1], Wen Dang [b,1], Zhengwang Shi [b], Mingyang Ding [b,c], Fan Xu [b], Tao Li [b], Tao Feng [b], Haixue Zheng [b,*], Shuqi Xiao [a,*]

[a] College of Veterinary Medicine, Northwest A&F University, Yangling, 712100, China
[b] State Key Laboratory of Veterinary Etiological Biology, College of Veterinary Medicine, Lanzhou University, Lanzhou Veterinary Research Institute, Chinese Academy of Agricultural Sciences, Lanzhou, 730046, China
[c] College of Veterinary Medicine, Gansu Agricultural University, Lanzhou, 730070, China

ARTICLE INFO

Keywords:
African swine fever virus (ASFV)
Multigene families (MGFs)
MGF505-2R
Differentially expressed genes (DEGs)

ABSTRACT

African swine fever (ASF) is etiologically an acute, highly contagious and hemorrhagic disease caused by African swine fever virus (ASFV). Due to its genetic variation and phenotypic diversity, until now, no efficient commercial vaccines or therapeutic options are available. The ASFV genome contains a conserved middle region and two flexible ends that code for five multigene families (MGFs), while the biological functions of the MGFs are not fully characterized. Here, ASFV MGF505-2R-deficient mutant ASFV-Δ2R was constructed based on a highly virulent genotype II field isolate ASFV CN/GS/2018 currently circulating in China. Transcriptomic profiling demonstrated that ASFV-Δ2R was capable of inducing a larger number of differentially expressed genes (DEGs) compared with ASFV CN/GS/2018. Hierarchical clustering of up-regulated DEGs revealed that ASFV-Δ2R induced the most dramatic expression of interferon-related genes and inflammatory and innate immune genes, as further validated by RT-qPCR. The GO and KEGG pathway analysis identified significantly enriched pathways involved in pathogen recognition and innate antiviral immunity. Conversely, pharmacological activation of those antiviral immune responses by exogenous cytokines, including type I/II IFNs, TNF-α and IL-1β, exerted combinatory effects and synergized in antiviral capacity against ASFV replication. Collectively, MGF505-2R is a newly identified inhibitor of innate immunity potentially implicated in immune evasion.

1. Introduction

African swine fever (ASF) is a highly contagious infectious disease affecting both domestic pigs and wild boars. The mortality rates reach as high as 100% in domestic pig herds infected with highly virulent ASFV strains (Zhao et al., 2019). Up to now, no commercial vaccines or therapeutic drugs are available. Current control measures consisting of strict animal quarantine and culling procedures are costly and unachievable, especially for small holder farms, leading to a devastating hit to the pig industry around the world.

ASFV, the causative agent of AFV, is the sole DNA arbovirus of the family A*sfarviridae*. ASFV is a group of icosahedral double-stranded DNA viruses belonging to the nucleo-cytoplasmic large DNA viruses (NCLDV). Its genome is ranging from 170 to 193 kb in length, with variation being dominantly derived from the gain or loss of numbers of multigene families (MGFs) located in terminal variable regions. Until now, at least five MGFs have been identified, namely MGF100, MGF110, MGF300, MGF360 and MGF530/505, in which MGF360 and MGF505 have been widely proved to determine ASFV host range and virus replication (Zsak et al., 2001; Vivian et al., 2015; Gladue et al., 2016; O'donnell et al., 2016). Noticeable is the fact that MGF360 and MGF505 share partial sequence and structural identities (Vivian et al., 2015). Thus, advances in one are presumably contributable to accelerating the research of the other, especially in the subject of host range specificity, virus virulence and blocking of the host innate immune response (Zsak et al., 2001; Afonso et al., 2004; Vivian et al., 2015; Gladue et al., 2016). It has been reported that deleting *MGF360* and *MGF505* genes in the cell culture-adapted, highly attenuated ASFV variants MS16 and BA71V conferred deficiency in replication in swine macrophage cell cultures (Zsak et al., 2001; Zsak and Neilan, 2002). In addition, studies had shown

* Corresponding authors.
E-mail addresses: haixuezheng@163.com (H. Zheng), xiaoshuqi@nwsuaf.edu.cn (S. Xiao).
[1] Huaguo Huang and Wen Dang contributed equally to this work.

https://doi.org/10.1016/j.virs.2022.11.009
Received 5 May 2022; Accepted 22 November 2022
Available online 25 November 2022
1995-820X/© 2022 The Authors. Publishing services by Elsevier B.V. on behalf of KeAi Communications Co. Ltd. This is an open access article under the CC BY-NC-ND license (http://creativecommons.org/licenses/by-nc-nd/4.0/).

the *MGF360* and *MGF505* genes were essential for virus replication and generation of infection in *Ornithodoros* porcinus ticks (Burrage et al., 2004). Very recently, MGF505-7R was reportedly capable of inhibiting the production of IL-1β and type I IFNs through interrupting inflammasome formation and blocking the nuclear translocation of IRF3, respectively (Li J. et al., 2021b). In parallel, MGF505-7R negatively regulated both cGAS-STING-mediated signaling pathway and proinflammatory IFN-γ-mediated JAK-STAT signaling (Li D. et al., 2021b; Li D. et al., 2021d). Moreover, MGF360-9L was identified as a major virulence factor associated with ASFV pathogenesis by antagonizing the JAK/STAT signaling pathway (Zhang et al., 2022).

MGF505-2R had been documented to inhibit IL-1β maturation and IFN-β promoter activation (Li J. et al., 2021a). However, the exact cellular signaling pathways that were fine-tuned by MGF505-2R during the process of ASFV infection were not fully elucidated. To this aim, ASFV MGF505-2R-deficient mutant, namely ASFV-Δ2R was constructed based on a highly virulent genotype II strain ASFV CN/GS/2018 currently circulating in China. RNA-seq was employed to reveal the gene expression profile changes of bone marrow-derived macrophage (BMDM) exposed with same amount of ASFV CN/GS/2018 or ASFV-Δ2R. High-resolution profile of transcriptomes reveals substantial up-regulation of genes related to host antiviral immunity, highlighting the role of MGF505-2R on immune evasion. Pharmacological activation of representative signaling pathways, including JAK-STAT pathway, TNF-α signaling pathway and interleukin-1β (IL-1β) pathway exerts synergistically inhibitory effects against ASFV replication. Our results lay foundation basis for decoding the function of MGF505-2R and rational design of genetically manipulated live attenuated vaccine against ASF infection.

2. Materials and Methods

2.1. Cells, viruses and reagents

HEK293T cells were purchased from ATCC and cultured in Dulbecco's modified Eagle's medium (DMEM) (GIBCO, Invitrogen China Limited, Shanghai, China) supplemented with 10% (v/v) fetal bovine serum (FBS) (BI, Biological Industries Israel Beit Haemek LTD., Kibbutz Beit-Haemek, Israel) and 1% penicillin-streptomycin (100 IU/mL penicillin, 5 mg/L streptomycin) (GIBCO). ASF strain ASFV CN/GS/2018, a genotype II strain currently circulating in China, was characterized and preserved in our lab. Human IFN-α 1b (Cat# Z02866-10), IFN-α 2a (Cat# Z03003-50), IFN-β (Cat# Z03109-25) and IFN-γ (Cat# Z02986-50) were purchased from GenScript (Nanjing, China) and reconstituted in PBS containing 0.1% BSA at 50 μg/mL. Recombinant porcine IL-1β (Cat# P6452) was purchased from Beyotime (Shanghai, China) and TNF-α (Cat# HY-P7302) was purchased from MCE (MedChemExpress). GM-CSF (Cat# G5035) and mouse anti-Flag monoclonal antibody (Cat# F1804) were purchased from Sigma-Aldrich. Anti-mouse IgG (Alexa Fluor® 488 conjugate) (Cat# 4408) secondary antibody was purchased from Cell Signaling Technology (Danvers, MA, USA).

2.2. Preparation of bone marrow-derived macrophage (BMDM)

The collection of bone marrow cells from the femur and tibia of 4-week-old pigs was performed as previously described with minor modifications (Carrasco et al., 2001; Kim et al., 2019). After resuspending and filtering through a 100 μm cell strainer, bone marrow cell cultures were plated into bacteria Petri dishes (10 cm) at approximately 0.5×10^7 live cells per dish. Then bone marrow culture medium was added with 1 ng/mL of GM-CSF (10 mL/dish) and culture at 37 °C, 5% CO_2. Half volume of the same growth medium was replenished on day 4. Following 7-day of differentiation, for creating a cell suspension, cells were dislodged using a cell scraper to create cell suspension, then washed and resuspended in bone marrow culture medium. The obtained BMDM cells were cryopreserved at −80 °C at a concentration of 1.0×10^7 cells per vial. Before use, the frozen BMDM cells were thawed and plated into a multi-well plate with approximately 80% confluence.

2.3. Detection of MGF505-2R transcription and cellular localization of its encoded protein

The transcriptional kinetics of MGF505-2R were assessed by reverse transcription-quantitative PCR (RT-qPCR) along with the early CP204L (*p30*) and late B646L (*p72*) expressed genes of ASFV as reference genes. In detail, BMDM were infected with ASFV CN/GS/2018 at a low MOI of 0.1. For indicated duration, namely 3 h, 6 h, 9 h, 12 h, 15 h and 18 h post infection, representing an approximately one life cycle of ASFV replication, then total RNA was extracted from cell cultures using a RNeasy mini kit (Qiagen, USA) according to the manufacturer's instructions. The RNA was further subjected to RT-qPCR.

Determining the sub-cellular localization of a protein within a cell is often an essential step towards understanding its function. To this aim, expression-ready MGF505-2R cDNA ORF clone with enhanced promoter in expression vector (p3XFLAG-CMV™-10 expression vector) was designed and confirmed by full-length sequence. A total of 2 μg of plasmid or backbone vector (CTR) was transfected into HEK293T adherent cells with JetPRIME® (Polyplus transfection, France; Cat# PT-114–15). After 24 h culture, immunofluorescence staining of cells with mouse anti-Flag tag monoclonal antibody (Sigma-Aldrich, USA; Cat# F1804) was performed with DAPI (10 μg/mL; Solarbio) as a useful stain for nuclear quantitation. To clarify whether subcellular location alteration of MGF505-2R-encoded protein occurred in response to ASFV DNA invasion, cells were initially transfected with HT-DNA (Sigma-Aldrich) at 2 μg per well. Following 24 h incubation, cells were further exposed to MGF505-2R overexpression plasmid for immunofluorescence staining.

2.4. Construction and characterization of ASFV MGF505-2R-deficient mutant ASFV-Δ2R

ASFV deficient in the *MGF505-2R* gene was constructed by homologous recombination using a recombinant transfer vector pASFV-Δ2R as described elsewhere. In detail, pASFV-Δ2R carries an eGFP reporter gene cassette under the control of ASFV *p72* late gene promoter flanked with left arm of 1000 bp upstream of MGF505-2R (corresponding to 32,122–33,121 bp) and right arm of 1000 bp downstream of MGF505-2R (corresponding to 34,703–35,702 bp). As designed, this construction resulted in a 1581-nucleotide deletion as well as a 917-nucleotide eGFP insertion between nucleotide positions 33,121–34,702. Following successive rounds of limiting dilution purification based on eGFP activity detection, the purified ASFV-Δ2R recombinant virus was obtained and its homogeneity was determined by traditional PCR. In detail, two pairs of primers were designed, with one binding inside the *MGF505-2R* gene (referred to as centering primer) and the other binding outside (referred to as flanking primer) (Supplementary Table S1). The PCR products were subjected to DNA electrophoresis and Sanger sequencing was conducted for precise identification of genetic modifications in the ASFV-Δ2R.

To determine whether genetic deletion and eGFP insertion could fine-tune ASFV replication in a multi-step growth curve, BMDM were infected with ASFV CN/GS/2018 or ASFV-Δ2R at a low MOI (0.1). For indicated duration, namely 2 h, 24 h, 48 h, 72 h and 96 h post infection, whole cell cultures were harvested, repeatedly frozen thawed, and clarified by centrifugation at 12000 ×*g* for 10 min. Viral loads were titrated by $TCID_{50}$ assay or quantification of ASFV genomic copies using ASFV p72-specific Fluorescent quantitative PCR (FQ-PCR) (Forward: 5′-ACAAGCGTGTAAACGGCG-3'; Reverse: 5′-CTGGCAGGATGCTCCGAT-3'; TaqMan probe: FAM-GCTGCCCATGGGCCCCCATCTGGGA-TAMRA).

2.5. Next-generation sequencing of ASFV-Δ2R

Virus suspension was harvested from ASFV-Δ2R-infected BMDM cells, clarified, and ultracentrifugated. ASFV genomic DNA was extracted

from virus pellet using viral DNA kit (Omega, USA; Cat# D3892). The harvested DNA was detected by the agarose gel electrophoresis and quantified by Qubit 2.0 Fluorometer (Thermo Scientific, USA). The whole genome of ASFV-Δ2R was sequenced using Illumina NovaSeq Pe150 platform performed at the Beijing Allwegene Technology Co., Ltd. The SPAdes (v3.13.0) software (Bankevich et al., 2012) was used to assemble the paired reads into a number of scaffolds. Scaffolds with larger than 500 bp were aligned to reference sequence.

2.6. RNA extraction, library construction and data analysis

BMDM cells were exposed to ASFV CN/GS/2018 or ASFV-Δ2R at the MOI of 0.1. For indicated durations, total RNA was extracted using the mirVana miRNA Isolation Kit (Ambion) following the manufacturer's protocol. RNA integrity was evaluated using the Agilent 2100 Bioanalyzer (Agilent Technologies, Santa Clara, CA, USA). The samples with RNA Integrity Number (RIN) $\geq$ 7 were subjected to the subsequent analysis. The cDNA libraries were constructed using TruSeq Stranded mRNA LTSample Prep Kit (Illumina, San Diego, CA, USA) according to the manufacturer's instructions. Then these cDNA libraries were sequenced on the Illumina sequencing platform (HiSeqTM 2500 or Illumina HiSeq XTen) (illumine, San Diego, CA, USA) and 125 bp/150 bp paired-end reads were generated. The following transcriptome sequencing and analysis were performed by OE Biotech Co., Ltd. (Shanghai, China).

2.7. Validation of RNA-seq data with RT-qPCR

BMDM cells were infected with 0.1 MOI of ASFV CN/GS/2018 or ASFV-Δ2R in six-well plates. For indicated durations, whole cellar RNA was extracted with TRIzol reagent (Invitrogen, USA; Cat# 15,596,026) and subjected to reverse transcription using Prime Script RT reagent kit (Takara, Japan; Cat# RR037A) according to the manufacturer's instructions. The resulting cDNA was then used as the template for real-time qPCR using the TB Green Premix Ex Taq mix kit (Takara, Japan; Cat# RR402B). The results were depicted by the $2^{-\Delta\Delta Ct}$ method and expressed relative to the control sample (Schmittgen and Livak, 2008). All the RT-qPCR primers used were listed in Supplementary Table S2.

2.8. In vitro antiviral assay

BMDM cells at optimal concentration (approximately 70%–90% confluence) were infected with ASFV CN/GS/2018 at an MOI of 0.1. Following 2 h incubation, the residual virus inoculum was removed by repeated washing and cells were cultured in growth medium supplemented with different concentrations of cytokines. At 48 h post-treatment, the whole cultures were harvested following repeated freezing and thawing, then clarified and subjected to titration by $TCID_{50}$ assay.

2.9. Cell viability assay

Cell viability following cytokine stimulation was assessed with reagents and instructions provided by the Cell Counting Kit-8 (CCK-8) (Biosharp, China; Cat# BS350A). In brief, 5×10^4 BMDM cells were seeded into the 96-well plates. Following overnight culture, the plate was replenished with fresh growth medium supplemented with the same concentrations of cytokines as *in vitro* antiviral assay. At 24 h post-treatment, 10 μL of CCK-8 reagent was added to each well for 45 min incubation at 37 °C. The absorbance of each well was detected at a wavelength of 450 nm. The experiment was repeated for three times with two replicates in each experiment.

2.10. Statistical analysis

The significance of the results between the experiments was analyzed using GraphPad Prism 7 (San Diego, CA, USA). All data were presented as mean values ± standard errors (SEs) from three independent experiments. The *P* value was calculated by unpaired *t*-test, $^*P < 0.05$ was considered statistically significant. $^{**}P < 0.01$ and $^{***}P < 0.001$ were considered highly statistically significant.

3. Results

3.1. MGF505-2R is highly conserved especially in ASFV genotype I and II strains

The open reading frame (ORF) of MGF505-2R is located in the left variable region of ASFV CN/GS/2018 isolate, with nucleotide positions corresponding to 33,122 to 34,702 of its genome. It encodes an unstructured protein of dominantly 526 to 527 residues in length that lacks any functional annotations in Pfam (PFAM version 35.0). To assess the diversity of the MGF505-2R protein across multiple ASFV isolates, we conducted a pairwise comparison analysis of the degree of MGF505-2R conservation with strains in the African Swine Fever Virus Database (http://asfvdb.popgenetics.net/) by multiple-sequence alignment using compositionally adjusted substitution matrices (Supplementary Table S3). The identity between the 43 ASFV isolates and the WT ASFV was 81%–100% at the protein level, with the highest of 100% being observed in most of genotype II isolates, moderately high of 98%–99% in genotype I isolates and comparatively low of 81%–90% in the majority of isolates circulating in Sub-Saharan Africa. Of note, three isolates, namely Spain_E75_1975 (Genotype I, GenBank accession QED21648.1), China_ASFV-SY18_2018 (Genotype II, GenBank accession CBW46724.1), and Russia Odintsovo 2014 (Genotype II, GenBank accession CAN10124.1), showed a truncated C terminus that yielded a protein of 357, 357 and 332 amino acids in length, respectively (Supplementary Fig. S1). Meanwhile, 8 bp gaps were mainly observed in the genotype IX isolates (Supplementary Table S3). Three representative regions of ASFV MGF505-2R [Region 1 (aa 29–51), Region 2 (aa 169–185) and Region 3 (aa 410–434)] showed varied amino acid identities among different genotypes (Fig. 1). The alignment of complete MGF505-2R protein with other reference strains was demonstrated in Supplementary Fig. S1. Those data collectively revealed highly conservation of MGF505-2R sequences across different genotype I and II isolates.

3.2. Transcriptional kinetics of MGF505-2R and intracellular localization of its encoded protein

A time-course transcriptional kinetics of MGF505-2R were assessed in BMDM infected with ASFV CN/GS/2018, along with *CP204L* and *B646L* genes as representatives of early and late gene expression, respectively. At the very first beginning of 3 h post infection (hpi), MGF505-2R was highly expressed, paralleling the expression of CP204L and contrasting the expression of B646L. MGF505-2R expression progressively boosted and reached a plateau at 12 hpi, demonstrating gene expression patterns similar to *B646L* gene (Fig. 2A). Typically, the ASFV life cycle can be as quick as about 18 h (Zhu et al., 2019; Wang et al., 2021). It showed that MGF505-2R was highly transcribed throughout the virus replication cycle. Subsequently, we studied the intracellular localization of MGF505-2R protein by fusing the target gene with 3 × FLAG peptide, as per the deficiency in commercially available antibodies specific for MGF505-2R-encoded protein. Compared to mock-transfected cells (Fig. 2B, upper), our results demonstrated clearly that MGF505-2R-encoded protein was abundant in cytosol and microtubule organizing center but excluded from the nucleoli (Fig. 2B, middle) in transiently overexpressed HEK293T cells. It is reported that ASFV is capable of activating STING during virus infection, resulting in the full activation of an innate immune response to DNA viruses (Raquel et al., 2019; Razzuoli et al., 2020; Liu et al., 2021). In the present study, HEK293T cells were initially stimulated with exogenous HT-DNA before transfection so as to mimic ASFV DNA. As anticipated the presence of dsDNA-induced innate immune response could not shift the localization

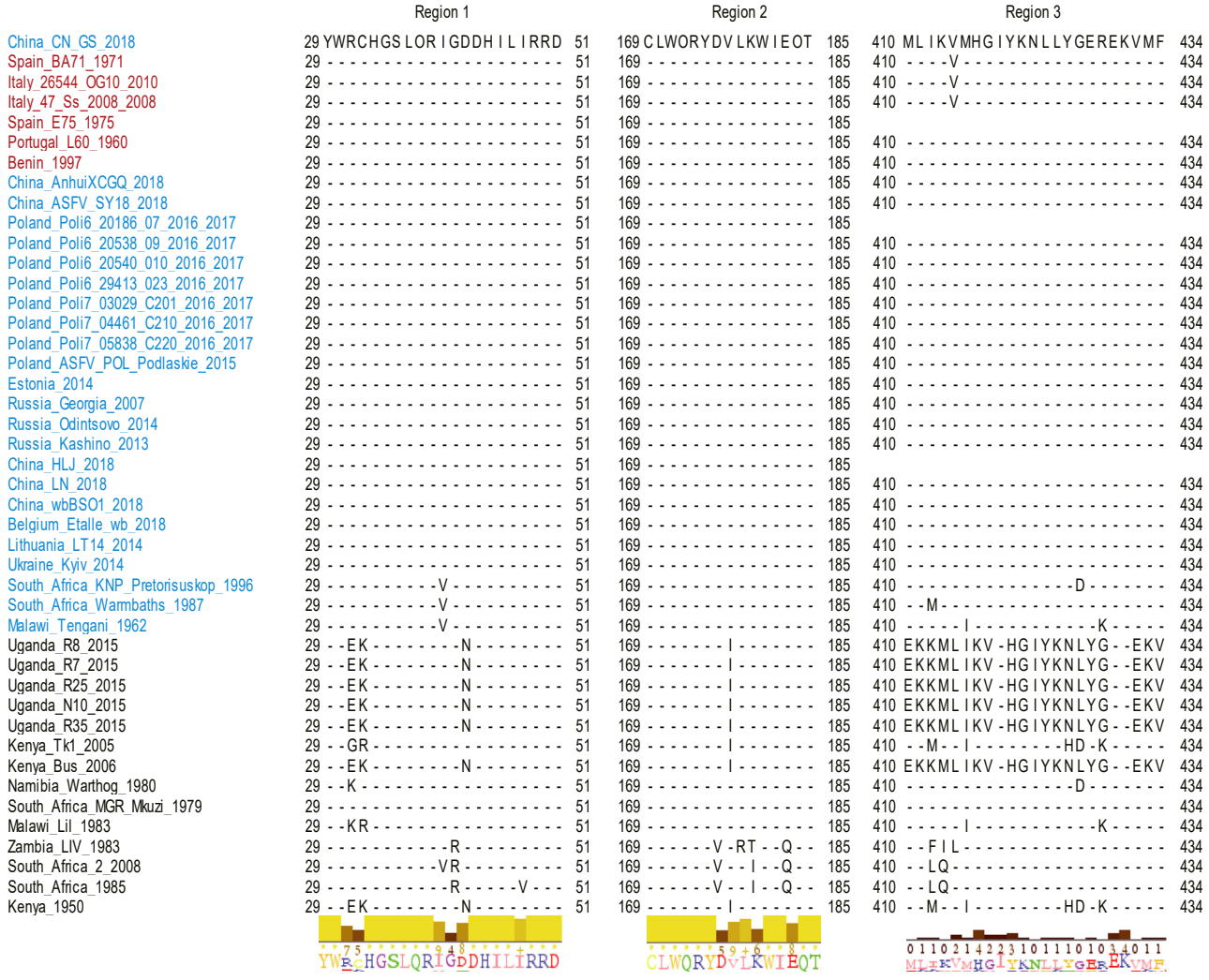

Fig. 1. Multiple sequence alignment of viral protein encoded by *MGF505-2R* gene. Three representative regions of Region 1 (aa 29–51), Region 2 (aa 169–185), and Region 3 (aa 410–434) were shown. Strains with red font indicate the isolates from genotype I and blue font indicate the isolates from genotype II. Other genotypes are indicated by black font. Forty-four protein sequences representing the genetic diversity of gene *MGF505-2R* of ASFV at ASFVdb (The African Swine Fever Virus Database (popgenetics.net)) were included to perform this alignment with ASFV CN/GS/2018. The results were depicted below the sequences as conservation histogram and consensus logo, with matching residues represented as periods and gaps in the sequence represented by dashes. The complete amino acid sequence alignments of MGF505-2R protein were shown in Supplementary Fig. S1.

of MGF505-2R-encoded protein (Fig. 2B, lower). We observed the same findings in HeLa cells (Supplementary Fig. S2).

3.3. Construction and characterization of recombinant MGF505-2R-deficient mutant ASFV-Δ2R

For generation of recombinant MGF505-2R-deficient mutant, a transfer plasmid containing the eGFP ORF under transcriptional control of the *p72* promoter flanked by segments of MGF505-2R gene, referred to as pASFV-Δ2R was applied to the following procedures (Fig. 3A). The pASFV-Δ2R was transiently transfected into fresh BMDM followed by infection with ASFV CN/GS/2018 at an MOI of 0.5. Autofluorescing foci of rounded and granulated cells were indicative of productive replication of recombinant virus. Cells from autofluorescing foci were collected by aspiration and re-inoculated onto fresh BMDM (Fig. 3B). Following a series of passage and purification, homogeneity of ASFV-Δ2R was assessed by traditional PCR. Using primer pair targeting the MGF505-2R gene (also referred to as centering primer, Supplementary Table S1), our PCR assays revealed that no wild type virus genomes were detectable in ASFV-Δ2R-infected BMDM (Fig. 3C; Fig. 3D, left panel), suggesting that the recombinant virus stock was essentially free from contaminating ASFV CN/GS/2018. Of note, by using primer pair flanking the MGF505-2R gene (also referred to as flanking primer, Supplementary Table S1), our PCR assays demonstrated differential bands in ASFV CN/GS/2018- and ASFV-Δ2R-infected BMDM (Fig. 3C; Fig. 3D, right panel).

To confirm the genetic identities, the PCR products were subjected to Sanger sequencing. The results were consistent with the intended modifications (Supplementary Fig. S3). Besides, next-generation sequencing of ASFV-Δ2R genome was performed to detect the emergence of unwanted additional mutations outside MGF505-2R. Following a full-length genome comparison in relation to ASFV CN/GS/2018, ASFV-Δ2R demonstrated the following genomic changes: the presence of four nucleotide insertions (an A nucleotide insertion, a C nucleotide insertion, a G nucleotide insertion and a GG nucleotide insertion at nucleotide positions 102, 430, 16,664 and 20,835, respectively) and five nucleotide deletions (three A nucleotide deletions at 794, 7226 and 175,676, respectively; a GGGGG nucleotide deletion and a T nucleotide deletion at

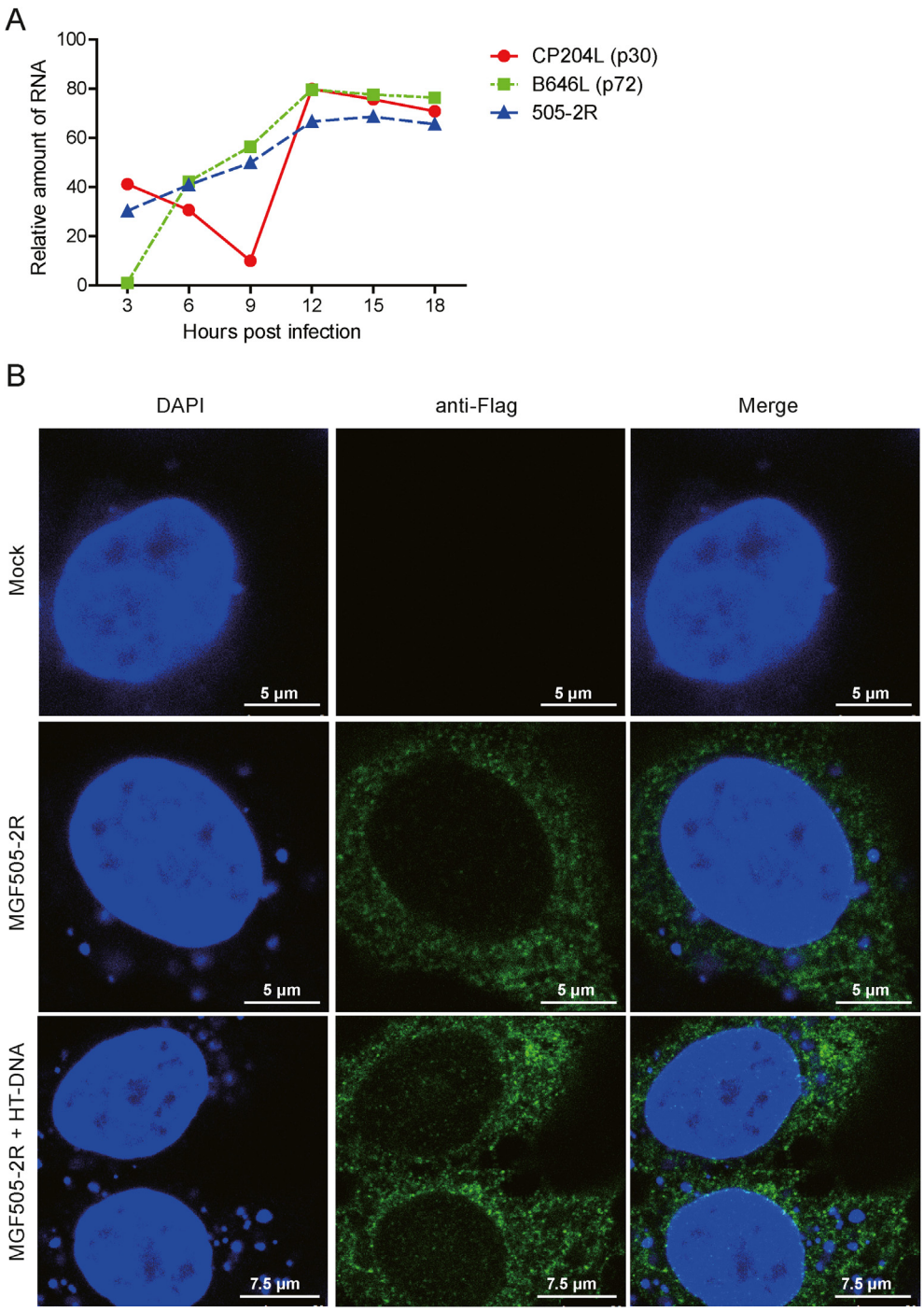

Fig. 2. Transcriptional kinetics of MGF505-2R and intracellular localization of its encoded protein. **A** Basic transcriptional changes of genes *MGF505-2R*, *CP204L*, *B646L* within 18 h, representing an approximate one life cycle of ASFV replication. The results at the indicated time points were expressed relative to the values at 0 hpi by using the $2^{-\Delta\Delta Ct}$ method. Data are expressed as mean ± standard error of the mean of four replicate samples. **B** The HEK293T cells were mock-transfected (top) or transiently transfected with 2 μg of MGF505-2R plasmid. Fluorescence microscopy was applied to visualize the localization of its encoded protein after 24 h transfection. To mimic ASFV infection, HEK293T cells were primarily stimulated with 2 μg HT-DNA and subsequently transfected with the same amount of MGF505-2R overexpression plasmid. Cell nuclei were stained with DAPI.

positions 19,032 and 54,525, respectively) in the noncoding regions (NCR); a residue substitution (Asp to Pro) at residue position 455 in ORF M1249L and three residue substitutions (Ser to Gly, Phe to Arg and Ser to Gly) at residue positions 110, 75, 67 in ORF O174L (Table 1). Whether and how those unwanted genetic changes affect the phonotype of ASFV-Δ2R awaits further investigation.

Assessment of replication kinetics demonstrated that, irrespective of detection methods used, the mutant revealed similar growth kinetics as ASFV CN/GS/2018 at the early stage of infection, but produced relatively lower viral titers starting as early as 48 hpi (Fig. 3E). Those data concluded that MGF505-2R-deletion and eGFP-insertion slightly attenuated *in vitro* replication of ASFV-Δ2R.

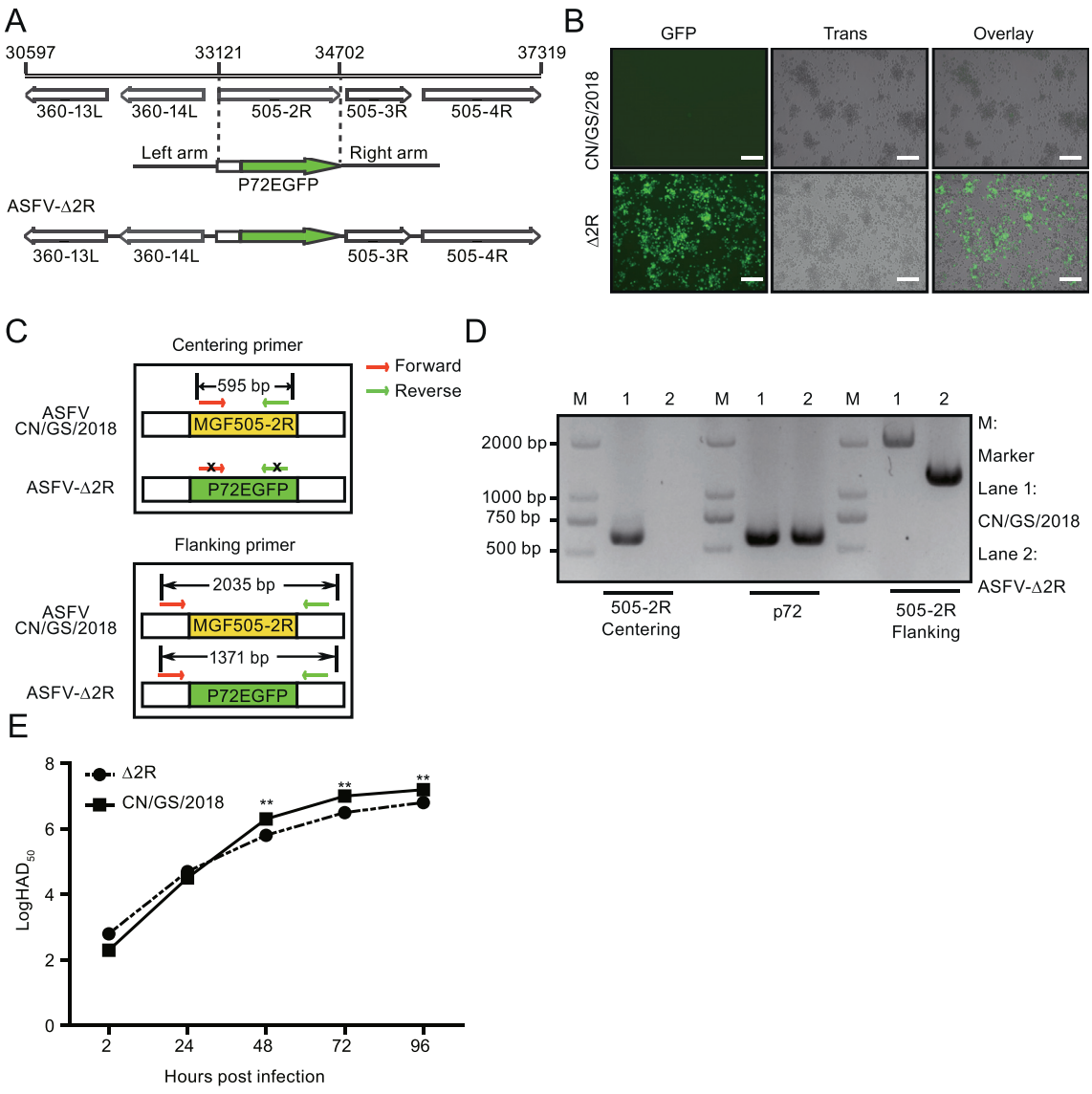

Fig. 3. Construction and assessment of recombinant ASFV-Δ2R mutant. **A** The construction strategy of recombinant ASFV-Δ2R mutant. **B** Fluorescence microscopy of BMDM infected with ASFV CN/GS/2018 or ASFV-Δ2R at an MOI of 0.1 for a duration of 24 h. Images were taken at 20x magnification. Scale bar = 300 μm. **C** Schematic demonstration of designing two pairs of primer with centering primer and flanking primer locating within and outside the MGF505-2R, respectively. The expected size of the PCR products is labeled. **D** The purity and insert sequence identification of recombinant ASFV-Δ2R mutant. A pair of primer targeting *p72* was employed as an indicator of ASFV genome input. **E** Comparison of virus particles in ASFV-Δ2R mutant and ASFV CN/GS/2018 infected BMDM. BMDM were infected with ASFV-Δ2R mutant or wild type at an MOI of 0.1. At the indicated time points, whole cell cultures were freezed and thawed, clarified and subjected to $TCID_{50}$ titration for viable virus particles. $^{**}P < 0.01$.

3.4. Analysis of differentially expressed genes (DEGs) from ASFV CN/GS/2018 or ASFV-Δ2R-infected BMDM

To detail the gene expression profile changes associated with deletion of MGF505-2R, BMDM pre-infected with 0.1 MOI of ASFV CN/GS/2018 or ASFV-Δ2R for 18 h, and then the cells were subjected to RNA-seq. The results of TopHat alignment demonstrated that over 40 million 75 bp paired-end reads were generated for each sample, with a minimum of 76.81% of reads mapped successfully to the pig reference genome (v11.1) in ASFV-Δ2R-infected samples. Using strict criteria for differentially expressed genes (DEGs) identification ($Log_2FC > 1$ or < -1, P value < 0.05, FKPM >1), in total, 737 genes, including 272 down-regulated and 465 up-regulated genes, were identified as being significantly differentially expressed between ASFV CN/GS/2018-infected sample (18 h) and mock sample (Fig. 4A, upper panel). In parallel, ASFV-Δ2R was capable of inducing slightly more DEGs with 258 down-regulated and 498 up-regulated. Specifically, in the context of up-regulated DEGs, higher overall fold-changes were observed in the ASFV-Δ2R-infected sample compared to ASFV CN/GS/2018 (Fig. 4A, lower panel). Collectively, ASFV-Δ2R was slightly more capable of inducing relatively more up-regulated DEGs with overall higher fold-changes.

MGF505-2R is competent in inhibiting IL-1β and IFN-β production by using cell-based functional dual-reporter screening system, implying the involvement of MGF505-2R in immune evasion (Li J. et al., 2021b). In a more focused analysis of innate immune gene expression, our heatmap of innate immune-related DEGs demonstrated that ASFV CN/GS/2018 infection induced substantial elevation in transcript abundance of innate immune genes, with expression kinetics increasing as early as 6 h, peaking at 18 h and subsiding at 30 h. As anticipated, 18 h exposure to ASFV-Δ2R resulted in the most marked increase in expression of innate immune-related genes (Fig. 4B). In detail, ASFV-Δ2R infection boosted very high transcriptional induction of IFN-induced genes, such as interferon-stimulated gene 15 (ISG15), HECT and RCC1-containing

Table 1
Summary of differences between the full length genome sequence of ASFV-Δ2R and ASFV CN/GS/2018.

Nucleotide position[a]	Description of modification
102	Insertion of A (noncoding region)
430	Insertion of C (noncoding region)
16,664	Insertion of G (noncoding region)
20,835	Insertion of GG (noncoding region)
797	Deletion of A (noncoding region)
7226	Deletion of A (noncoding region)
19,032	Deletion of GGGGG (noncoding region)
54,525	Deletion of T (noncoding region)
175,676	Deletion of A (noncoding region)
78,094	M1249L, T to C (Asp455Pro)
128,448	O174L, A to G (Ser110Gly)
128,552	O174L, A to G (Phe75Ary)
128,577	O174L, A to G (Ser67Gly)

[a] , nucleotide position number based on the sequence of ASFV CN/GS/2018 strain.

protein 5 (HERC5), indoleamine 2, 3-dioxygenase 1 (IDO1), IFN-induced proteins with tetratricopeptide repeats (IFITs), interferon-inducible transmembrane (IFITM) proteins and UBE2L6 (Fig. 4B). Additionally, ASFV-Δ2R exhibited dramatic induction of genes crucial during the acute phase response, such as interleukin (IL)-1a, 1b, 1R2, 18 and 27, tumor necrosis factor (TNF)-α and one member of the complement pathway C1R. Finally, genes coding for chemokines were also strongly induced, including C–C motif chemokine ligand 3 like 1 (CCL3L1), 4 (CCL4), 5 (CCL5) and 22 (CCL22) as well as C-X-C motif chemokine ligand 2 (CXCL2) and 10 (CXCL10) (Fig. 4B). Taken together, these data showed that ASFV-Δ2R resulted in stronger and more protracted induction of genes related to IFNs, inflammatory, and innate immune responses.

3.5. Validation of RNA-seq results by RT-qPCR

To verify transcriptomic changes obtained by RNA-seq dataset, a subset of genes that encode well-characterized key innate molecules of the antiviral responses were subjected to RT-qPCR analysis. As demonstrated in Fig. 5A, correspondingly, ASFV-Δ2R was more prominent in inducing innate immune gene expression changes relative to the ASFV CN/GS/2018, mirroring the results detected from RNA-seq. By comparing RNA-seq results and RT-qPCR data, we have found excellent correlation of gene expression patterns in ASFV CN/GS/2018-infected samples as well as in ASFV-Δ2R-infected samples, as demonstrated in Fig. 5B and C, respectively.

3.6. A robust innate response is mounted following ASFV-Δ2R infection for 18 h relative to ASFV CN/GS/2018

Since both ASFV CN/GS/2018 and ASFV-Δ2R are competent in activating antiviral innate immune responses, our differential analyses were designed to delineate transcriptional changes that are induced by ASFV-Δ2R infection relative to ASFV CN/GS/2018 (Fig. 6). Comparative analysis of the function of DEGs obtained from ASFV CN/GS/2018 and ASFV-Δ2R datasets revealed that, of the 357 up-regulated DEGs, several

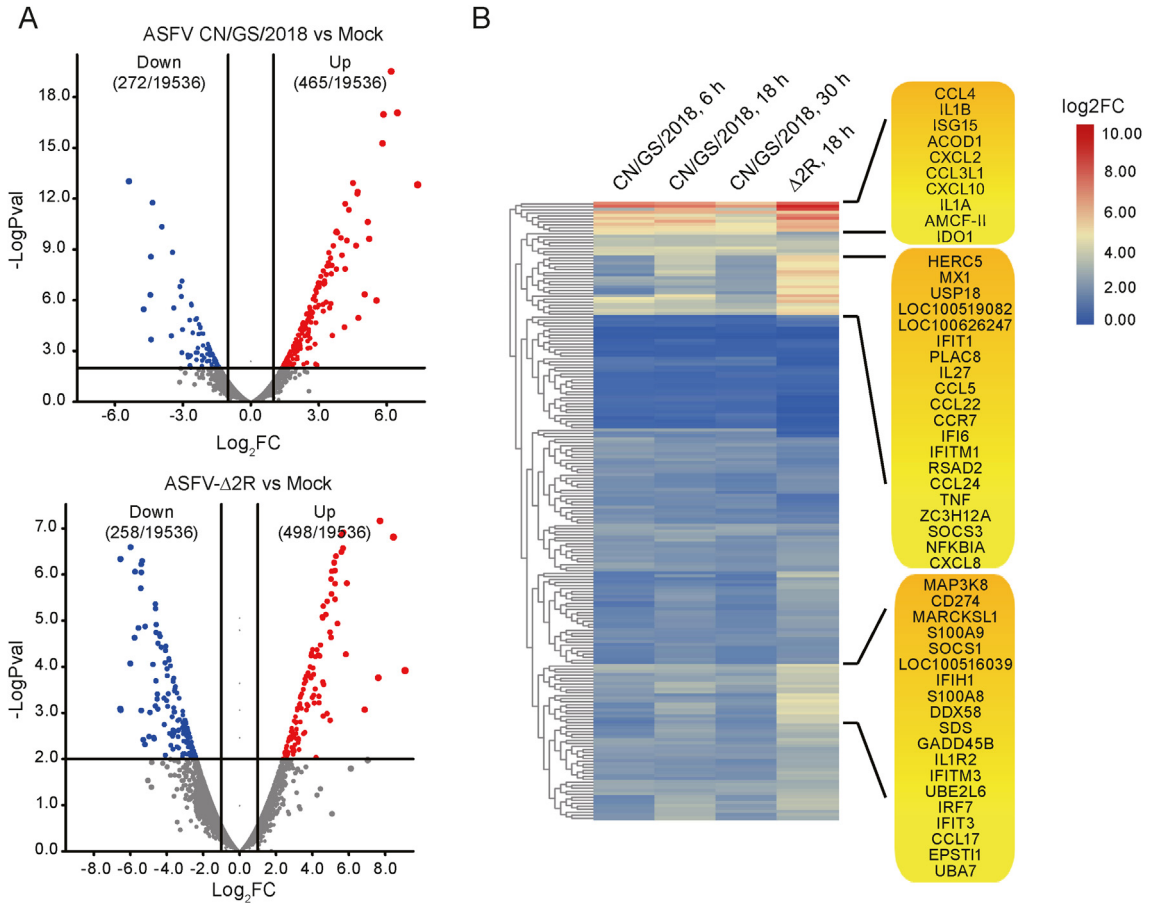

Fig. 4. Analysis of DEGs from ASFV CN/GS/2018 or ASFV-Δ2R-infected BMDM. **A** Volcano map of DEGs from ASFV CN/GS/2018- or ASFV-Δ2R-infected BMDM. The x-axis is the log2 scale of fold change of gene expression relative to mock sample. The y-axis is the minus log10 scale of the adjusted *P* values, which indicates the significant level of expression difference. The red dots represent significantly upregulated DEGs, while the blue dots represent significantly downregulated DEGs. Instead, grey dots represent genes unchanged. **B** Cluster analysis of DEGs involved in the innate immune response obtained from BMDM exposed to ASFV CN/GS/2018 at 6, 18 and 30 h infection, or ASFV-Δ2R at 18 h infection.

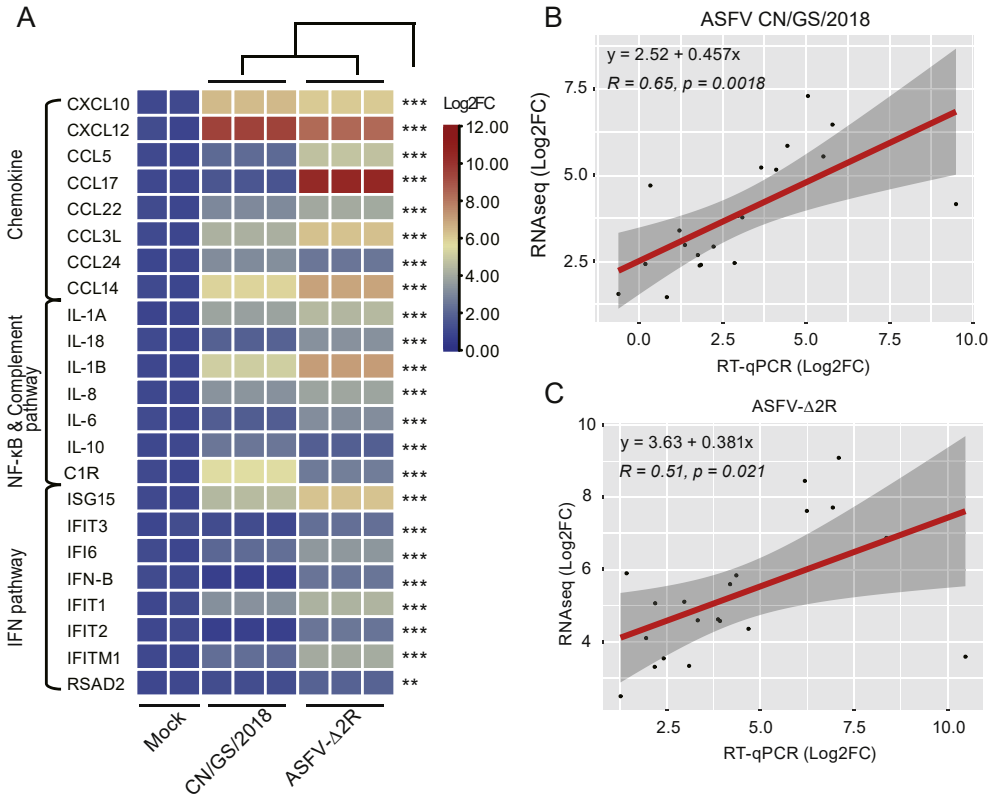

Fig. 5. Validation of RNA-seq results with RT-qPCR. **A** RT-qPCR analysis of the expression of indicated genes in BMDM pre-infected with ASFV CN/GS/2018 or ASFV-Δ2R at MOI of 0.1 for 18 h duration. The results were calculated by $2^{-\Delta\Delta Ct}$ method using porcine *GAPDH* as the reference gene. Data are presented as mean of two to three independent experiments with triplicate each. **B**, **C** Correlation analysis between RT-qPCR and RNA-seq data in ASFV CN/GS/2018-infected sample and ASFV-Δ2R-infected sample.

biological functions related to the immune and defense responses, including response to virus (15/357), defense response to virus (15/357), immune response (14/357), type I interferon signaling pathway (10/357) and negative regulation of viral genome replication (10/357) were significantly enriched (Fig. 6A). Instead, few GO terms were enriched by the down-regulated DEGs. Those biological functions along with GO terms represented in the cellular component (CC) and molecular function (MF) collectively shaped the landscape of host response to ASFV-Δ2R, especially those involved in the immune and defense response.

Similarly, KEGG pathway enrichment was also performed to identify cellular pathways altered by ASFV-Δ2R infection relative to ASFV CN/GS/2018 (Fig. 6B). Paralleling the findings in the GO analysis, in relation to ASFV CN/GS/2018, genes up-regulated by ASFV-Δ2R were predominantly involved in immune signaling pathways, including those crucial for viral recognition, namely RIG-I-like receptor signaling pathway, Toll-like receptor signaling pathway, NOD-like receptor signaling pathway and cytosolic DNA-sensing pathway, which were believed to play an integral role in the detection of ASFV and initiation of intracellular pathways. Correspondingly, several well-characterized classic antiviral pathways were also highly over-represented, including JAK-STAT signaling pathway TNF signaling pathway, TGF-β signaling pathway and chemokine signaling pathway.

3.7. Pharmacological activation of classic antiviral immune response inhibited ASFV replication

To explore the role of classic antiviral immune response on ASFV replication, a subset of exogenous cytokines, including type I/II IFNs, TNF-α and IL-1β were applied to *in vitro* antiviral assay against ASFV CN/GS/2018. Firstly, cytotoxicity of those cytokines was measured using the CCK-8 assay. As demonstrated in Supplementary Fig. S4, except for IFN-α 1b, which slightly but not significantly decreased the viability of BMDM cells, the rest of cytokines were non-cytotoxic and even elevated cell viability to a certain extent at the tested concentrations. IFN-β (type I IFN) and IFN-γ (type II IFN) exerted moderate to potent antiviral activity against ASFV by decreasing viral titers by approximately $10^{2.5}$ and 10^{4} $TCID_{50}$, respectively (Fig. 7A). Surprisingly, TNF-α and IFN-α 2a only slightly reduced ASFV replication, whereas IL-1β and IFN-α 1b had no major effect on ASFV replication. To clarify whether combination of cytokines could synergize in antiviral capacity, our results demonstrated that simultaneous treatment with TNF-α and type I IFN, as well as IL-1β and type I IFNs exerted a moderately synergistic antiviral effect against ASFV replication (Fig. 7B and C).

4. Discussion

African swine fever is notorious for constituting a socio-economic burden and a threat to global swine industry due to high tenacity, high case-fatality rate and the myriad of transmission routes. ASF continues to spread worldwide with emphasize on reappearance in the Americas (July 2021) and the Italian mainland (January 2022) after around 40 years of absence (Borca, 2021; Iscaro et al., 2022; Ravilov et al., 2022). This marks an urgent need for development of commercial vaccines against ASF. However, although substantial advances have been made recently in development of potential vaccines, at present prevention is dominantly relying on biosecurity measures, partially due to high complexity of the etiological agent ASFV.

ASFV is characterized with genetic diversity and phenotypic variation, the former as evidenced by various genomes from about 170 to 193

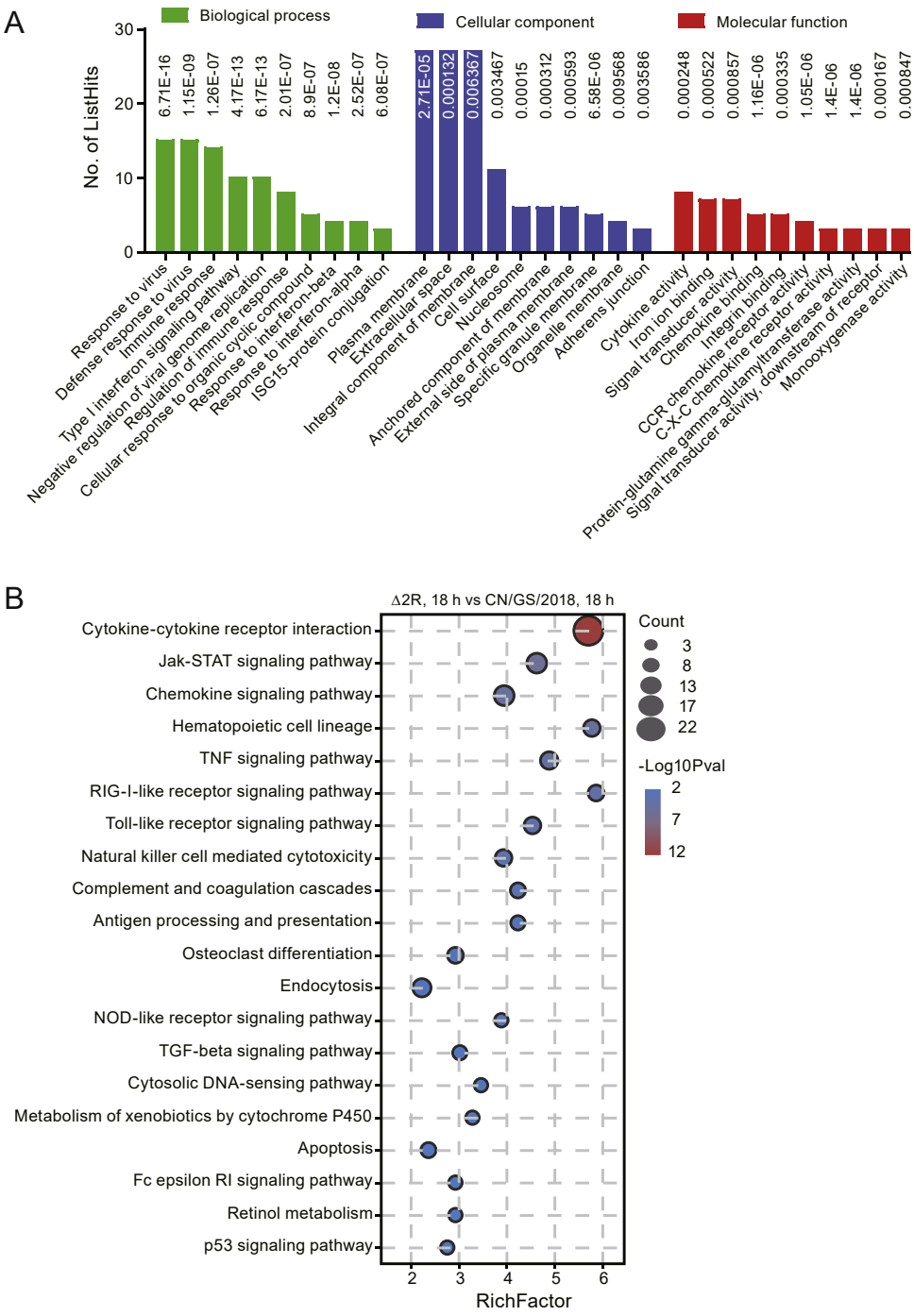

Fig. 6. GO and KEGG pathway enrichment analysis of DEGs in ASFV-Δ2R-infected sample relative to ASFV CN/GS/2018. **A** The gene numbers of top 10 GO terms of DEGs in biological process, cellular component and molecular function. The *P* value was labeled above the bars. **B** The top 20 pathways in KEGG enrichment analysis of DEGs.

bp in length and the latter as proven by 24 currently described genotypes based on the sequencing of the *B646L* gene. Until now, knowledge of the genomic characteristics of ASFV remains enigmatic. Comparative genomic analysis revealed that ASFV had an 'open' pan-genome. Of the 151–174 genes found in various ASFV strains, only 86 were identified as necessary genes, whereas the remains were flexible accessory genes (Wang et al., 2020). Significantly, ASFV MGFs of paralogous genes were characterized with gene duplication, sequence divergence, gene deletion and recombination, contributing to substantial variation in gene content relative to the rest of the genome. Variation in gene content can more readily result in profound changes in virus phenotype, further strengthening the notion that deletion of MGF is targetable for attenuation of ASFV (Malogolovkin and Kolbasov, 2019). Specifically deleting six genes belonging to MGF360 or MGF505: MGF505-1R, MGF360-12L, MGF360-13L, MGF360-14L, MGF505-2R and MGF505-3R, resulted in attenuation of highly virulent ASFV Georgia 2007isolate (ASFV-G) and conferred protection against a virulent homologous challenge (O'donnell et al., 2015). Similarly, same deletions of MGF360 and MGF505 genes in the virulent ASFV isolate Benin 97/1 resulted in the same effect (Reis et al., 2016). Very recently, combinational deletions of MGF360/505 and CD2v genes in Chinese ASFV HLJ/18 generated a safe and effective lie attenuated vaccine HLJ/18-7GD. It turned out to be fully attenuated,

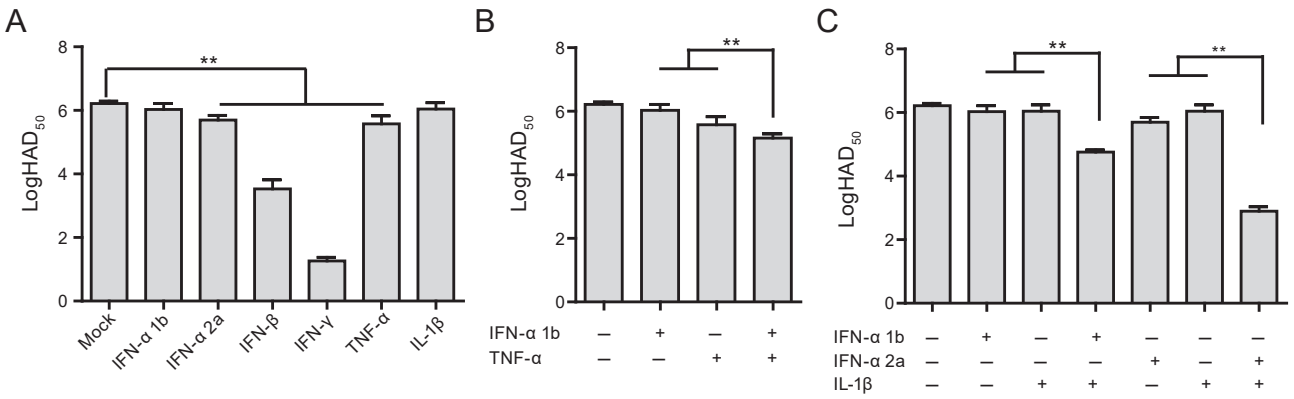

Fig. 7. The single and combinatory antiviral effects of cytokines on ASFV replication. **A** The antiviral effects of single cytokine on ASFV replication. BMDM pre-infected with ASFV CN/GS/2018 (MOI = 0.1) were cultured in the presence of cytokines (1000 U/mL for IFN-α 1b, IFN-α 2a, IFN-β and IFN-γ; 10 ng/mL for IL-1β; 20 ng/mL for TNF-α). For 24 h duration, viral titers were determined by $TCID_{50}$ assay. **B**, **C** The combinatory effects of two cytokines after 48 h incubation were tested as above-mentioned and analyzed by $TCID_{50}$ assay. $^{**}P < 0.01$.

cannot convert to the virulent strain, and provided complete protection (Chen et al., 2020). Moreover, several MGF members, including MGF110-1L (Ramirezmedina et al., 2021), MGF110-9L (Li D. et al., 2021a), MGF360-1L (Ramirez-Medina et al., 2020), MGF360-9L and MGF505-7R (Li J. et al., 2021b) were proved to be major virulence factors associated with ASFV. Those data exclusively implied that ASFV strains harboring less copies of MGF were often associated with a less virulent phenotype, representing a promising strategy for developing live attenuated vaccine against ASFV infection.

However, how the *MGF* genes influenced ASFV pathogenesis is rarely reported. Accumulating investigations revealed a strong association between MGF and immunomodulation, especially the type I IFN pathway. Meanwhile, those results were mainly derived from cell-based dual-fluorescence reporter systems, involving solely the well-characterized innate immune signaling pathways. This mainstreaming strategy is helpful but deficient in revealing genome-wide transcriptome characterization and profiling in response to virus infection. In the present study, our comprehensive RNA-seq transcriptomic profiling in the BMDM in response to ASFV CN/GS/2018 vs ASFV-Δ2R infection is sufficient for deepening the comprehensive understanding of potential function of MGF505-2R. As anticipated, MGF505-2R is implicated in down-regulation of innate immune response essential for pathogen recognition and type I IFN signaling pathway. In particular, MGF505-2R is also a negative modulator of inflammatory signaling pathway and NF-κB signaling pathway.

Indeed, IFN-β could trigger cell death. However, it is all about concentrations used. We measured the cell viability following cytokine stimulation at the concentrations used in the antiviral assay. As expected, cytokines did no harm to cell viability. Those results were displayed in Supplementary Fig. S4. The antiviral activities of cytokines against ASFV were reported elsewhere (Golding et al., 2016; Fan et al., 2020; Razzuoli et al., 2020; Esparza I et al., 1988). Previous report demonstrated that bovine IFN-$\alpha_1$1 inhibited ASFV replication in both porcine monocytes and alveolar macrophages. Meanwhile, porcine IFN-γ triggered the most pronounced inhibition of ASFV replication. In contrast, bovine TNF-α did not show any inhibitory activity (Esparza I et al., 1988). Those findings were aligned with our observations. Fan et al. reported that 100 and 1000 U/mL doses of porcine IFN-α and IFN-γ exerted moderate to potent antiviral activities against ASFV strain SY18 strain in PAMs with a synergistic effect. Meanwhile, combined PoIFN-α and PoIFN-γ displayed a synergistic inhibition of viral loads in ASFV-challenged pigs, implying the potential of recombinant porcine IFNs as a new strategy for the prevention of ASF (Fan et al., 2020). In our study, it seems that ASFV possessed less sensitivity to IFN-α. First, to guarantee the reproducibility of the antiviral assay, in the present study, commercially available recombinant human IFN-α was used. Meanwhile, many factors determine the inhibitory effect of IFN-α, including ASFV strains used, host cells, inoculation dose and treatment time.

However, the molecular mechanism of immune evasion by MGF505-2R is not explored in this study and awaits further investigation. During ASFV infection, the DNA signaling pathway was activated to induce type I IFNs and other cytokines. In this process, the involvement of the adaptor protein STING and the transcription factor IRF3 is instrumental for triggering the downstream signaling cascades. So far, a subset of ASFV proteins regulating IFN production has been identified. MGF505-7R negatively regulated cGAS-STING-mediated IFN-β production by degrading STING via autophagy (Li D. et al., 2021c). With respect to STING degradation, the same effect was observed for MGF505-11R (Yang et al., 2021). Meanwhile, MGF505-7R suppressed NF-κB activation and bound to NLRP3 to down-regulate inflammasome formation, resulting in decreased IL-1β production. Moreover, MGF505-7R interacted with and inhibited the nuclear translocation of IRF3 to antoganize type I IFN production (Li J. et al., 2021b), which was also the case for E120R (Liu et al., 2021). Besides, TBK1, a central kinase in innate adaptor complexes linking activation of PRRs to mobilization of transcriptional factors, is frequently targeted by ASFV proteins, such as A137R (Sun et al., 2022), DP96R (Wang et al., 2018), and MGF360-11L (Yang et al., 2022). Meanwhile, the JAK-STAT pathway stimulated by type I IFNs could also be perturbed by the ASFV protein. In this regard, MGF505-7R promoted degradation of JAK1 and JAK2 (Li D. et al., 2021d), whereas MGF360-9L interacted with and degraded STAT1 and STAT2. We believe those findings will lay foundation for understanding the potential molecular mechanism of MGF505-2R-mediated immune evasion.

5. Conclusions

In summary, we characterized the function of ASFV *MGF505-2R* gene using RNA-Seq based transcriptomic analysis. Compared to ASFV CN/GS/2018, ASFV-Δ2R induced the most dramatic and sustained expression of type I IFNs and inflammatory and innate immune genes, potentializing MGF505-2R as a potent negative modulator of the innate immune response, especially the type I IFN signaling pathway. Our results open additional avenues for decoding the function of MGF members.

Ethics statement

The present experiments with ASFV were carried out within Biosafety level 3 (BSL3) Biocontainment Facility in Lanzhou Veterinary Research Institute (LVRI), Chinese Academy of Agricultural Science (CAAS), and approved by the Ministry of Agriculture and Rural Affairs. This study was conducted in strict accordance with the recommendations in the Guide

for the Care and Use of laboratory Animals of Ministry of Science and Technology of the People's Republic of China.

Author contributions

Huaguo Huang and Wen Dang: conceptualization, investigation, methodology, data curation, writing-original draft, writing-review, editing. Zhengwang Shi, Mingyang Ding, Fan Xu, Tao Li and Tao Feng: software, validation, visualization. Haixue Zheng and Shuqi Xiao: funding acquisition, supervision, and resources.

Conflict of interest

The authors declare no competing financial interest.

Acknowledgements

This research was supported by grants from the National Key R&D Program of China (2021YFD1801300), the Key-Area Research and Development Program of Guangdong Province (grant number 2019B020211003), the Chinese Academy of Agricultural Science and Technology Innovation Project (grants number CAAS-ZDRW202006 and CAAS-ASTIP-2021-LVRI), and Technology Major Projects of Gansu Province (20ZD7A006 and NCC0006), as well as funding from the director of Lanzhou Veterinary Research Institute (LVRI-SZJJ-202106).

Appendix A. Supplementary data

Supplementary data to this article can be found online at https://doi.org/10.1016/j.virs.2022.11.009.

References

Afonso, C.L., Piccone, M.E., Zaffuto, K.M., Neilan, J., Kutish, G.F., Lu, Z., Balinsky, C.A., Gibb, T.R., Bean, T.J., Zsak, L., Rock, D.L., 2004. African swine fever virus multigene family 360 and 530 genes affect host interferon response. J. Virol. 78, 1858–1864.

Bankevich, A., Nurk, S., Antipov, D., Gurevich, A.A., Dvorkin, M., Kulikov, A.S., Lesin, V.M., Nikolenko, S.I., Pham, S., Prjibelski, A.D., 2012. SPAdes: a new genome assembly algorithm and its applications to single-cell sequencing. J. Comput. Biol. 19, 455–477.

Borca, M.V., 2021. Evaluation of an ASFV RNA helicase gene A859L for virus replication and swine virulence. Viruses 14, 10.

Burrage, T.G., Lu, Z., Neilan, J.G., Rock, D.L., Zsak, L., 2004. African swine fever virus multigene family 360 genes affect virus replication and generalization of infection in Ornithodoros porcinus ticks. J. Virol. 78, 2445.

Carrasco, C.P., Rigden, R.C., Schaffner, R., Gerber, H., Neuhaus, V., Inumaru, S., Takamatsu, H., Bertoni, G., Mccullough, K.C., Summerfield, A., 2001. Porcine dendritic cells generated in vitro: morphological, phenotypic and functional properties. Immunology 104, 175–184.

Chen, W., Zhao, D., He, X., Liu, R., Wang, Z., Zhang, X., Li, F., Shan, D., Chen, H., Zhang, J., Wang, L., Wen, Z., Wang, X., Guan, Y., Liu, J., Bu, Z., 2020. A seven-gene-deleted African swine fever virus is safe and effective as a live attenuated vaccine in pigs. Sci. China Life Sci. 63, 623–634.

Esparza, I., González, Jc, E.V., 1988. Effect of interferon-alpha, interferon-gamma and tumour necrosis factor on African swine fever virus replication in porcine monocytes and macrophages. J. Gen. Virol. 69, 7.

Fan, W., Jiao, P., Zhang, H., Chen, T., Zhou, X., Qi, Y., Sun, L., Shang, Y., Zhu, H., Hu, R., Liu, W., Li, J., 2020. Inhibition of african swine fever virus replication by porcine type I and type II interferons. Front. Microbiol. 11, 1203.

Gladue, Douglas, P., Krug Peter, W., Carlson, Jolene, O'donnell, Vivian, 2016. African swine fever virus Georgia isolate harboring deletions of 9GL and MGF360/505 genes is highly attenuated in swine but does not confer protection against parental virus challenge. Virus Res. 221, 8–14.

Golding, J.P., Goatley, L., Goodbourn, S., Dixon, L.K., Taylor, G., Netherton, C.L., 2016. Sensitivity of African swine fever virus to type I interferon is linked to genes within multigene families 360 and 505. Virology 493, 154–161.

Iscaro, C., Dondo, A., Ruocco, L., Masoero, L., Giammarioli, M., Zoppi, S., Guberti, V., Feliziani, F., 2022. January 2022: index case of new african swine fever incursion in mainland Italy. Trans. Emerg. Dis. 69, 1707–1711.

Kim, S.E., Hwang, J.H., Kim, Y.K., Lee, H.T., 2019. Heterogeneity of porcine bone marrow-derived dendritic cells induced by GM-CSF. PLoS One 14, e0223590.

Li, D., Liu, Y., Qi, X., Wen, Y., Li, P., Ma, Z., Liu, Y., Zheng, H., Liu, Z., 2021a. African swine fever virus MGF-110-9L-deficient mutant has attenuated virulence in pigs. Virol. Sin. 36, 187–195.

Li, D., Yang, W., Li, L., Li, P., Ma, Z., Zhang, J., Qi, X., Ren, J., Ru, Y., Niu, Q., Liu, Z., Liu, X., Zheng, H., 2021b. African swine fever virus MGF-505-7R negatively regulates cGAS-STING-mediated signaling pathway. J. Immunol. 206, 1844–1857.

Li, D., Yang, W., Li, L., Li, P., Zheng, H., 2021c. African swine fever virus MGF-505-7R negatively regulates cGAS–STING-mediated signaling pathway. J. Immunol. 206, ji2001110.

Li, D., Zhang, J., Yang, W., Li, P., Ru, Y., Kang, W., Li, L., Ran, Y., Zheng, H., 2021d. African swine fever virus protein MGF-505-7R promotes virulence and pathogenesis by inhibiting JAK1- and JAK2-mediated signaling. J. Biol. Chem. 297, 101190.

Li, J., Song, J., Kang, L., Huang, L., Zhou, S., Hu, L., Zheng, J., Li, C., Zhang, X., He, X., Zhao, D., Bu, Z., Weng, C., 2021a. pMGF505-7R determines pathogenicity of African swine fever virus infection by inhibiting IL-1beta and type I IFN production. PLoS Pathog. 17, e1009733.

Li, J., Song, J., Kang, L., Huang, L., Zhou, S., Hu, L., Zheng, J., Li, C., Zhang, X., He, X., Zhao, D., Bu, Z., Weng, C., 2021b. pMGF505-7R determines pathogenicity of African swine fever virus infection by inhibiting IL-1β and type I IFN production. PLoS Pathog. 17, e1009733.

Liu, H., Zhu, Z., Feng, T., Ma, Z., Xue, Q., Wu, P., Li, P., Li, S., Yang, F., Cao, W., Xue, Z., Chen, H., Liu, X., Zheng, H., 2021. African swine fever virus E120R protein inhibits interferon beta production by interacting with IRF3 to block its activation. J. Virol. 95, e0082421.

Malogolovkin, A., Kolbasov, D., 2019. Genetic and antigenic diversity of African swine fever virus. Virus Res. 271, 197673.

O'donnell, V., Holinka, L.G., Gladue, D.P., Sanford, B., Krug, P.W., Lu, X., Arzt, J., Reese, B., Carrillo, C., Risatti, G.R., Borca, M.V., 2015. African swine fever virus Georgia isolate harboring deletions of MGF360 and MGF505 genes is attenuated in swine and confers protection against challenge with virulent parental virus. J. Virol. 89, 6048–6056.

O'donnell, V., Holinka, L.G., Sanford, B., Krug, P.W., Carlson, J., Pacheco, J.M., Reese, B., Risatti, G.R., Gladue, D.P., Borca, M.V., 2016. African swine fever virus Georgia isolate harboring deletions of 9GL and MGF360/505 genes is highly attenuated in swine but does not confer protection against parental virus challenge. Virus Res. 221, 8–14.

Ramirez-Medina, E., Vuono, E.A., Rai, A., Pruitt, S., Silva, E., Velazquez-Salinas, L., Zhu, J., Gladue, D.P., Borca, M.V., 2020. Evaluation in swine of a recombinant african swine fever virus lacking the MGF-360-1L gene. Viruses 12, 1193.

Ramirezmedina, E., Vuono, E., Pruitt, S., Rai, A., Silva, E., Espinoza, N., Zhu, J., Velazquezsalinas, L., Borca, M.V., Gladue, D.P., 2021. Development and in vivo evaluation of a mgf110-1L deletion mutant in african swine fever strain Georgia. Viruses 13, 286.

Raquel García-Belmonte, Daniel, Pérez-Núñez, Marco, Pittau, Juergen, Richt, Yolanda, 2019. African swine fever virus Armenia/07 virulent strain controls IFN-β production through cGAS-STING pathway. J. Virol. 93, e02298–18.

Ravilov, R.K., Rizvanov, A.A., Mingaleev, D.N., Galeeva, A.G., Zakirova, E., Shuralev, E.A., Rutland, C., Khammadov, N.I., Efimova, M.A., 2022. Viral vector vaccines against ASF: problems and prospectives. Front. Vet. Sci. 9, 830244.

Razzuoli, E., Franzoni, G., Carta, T., Zinellu, S., Amadori, M., Modesto, P., Oggiano, A., 2020. Modulation of type I interferon system by african swine fever virus. Pathogens 9, 361.

Reis, A.L., Abrams, C.C., Goatley, L.C., Netherton, C., Chapman, D.G., Sanchez-Cordon, P., Dixon, L.K., 2016. Deletion of African swine fever virus interferon inhibitors from the genome of a virulent isolate reduces virulence in domestic pigs and induces a protective response. Vaccine 34, 4698–4705.

Schmittgen, T.D., Livak, K.J., 2008. Analyzing real-time PCR data by the comparative C(T) method. Nat. Protoc. 3, 1101–1108.

Sun, M., Yu, S., Ge, H., Wang, T., Li, Y., Zhou, P., Pan, L., Han, Y., Yang, Y., Sun, Y., Li, S., Li, L.F., Qiu, H.J., 2022. The A137R protein of african swine fever virus inhibits type I interferon production via the autophagy-mediated lysosomal degradation of TBK1. J. Virol. 96, e0195721.

Vivian, O'donnell, Holinka, Lauren, G., Gladue, Douglas, P., Sanford, Brenton, Krug, Peter, W., 2015. African swine fever virus Georgia isolate harboring deletions of MGF360 and MGF505 genes is attenuated in swine and confers protection against challenge with virulent parental virus. J. Virol. 89, 6048–6056.

Wang, L., Luo, Y., Zhao, Y., Gao, G.F., Bi, Y., Qiu, H.J., 2020. Comparative genomic analysis reveals an 'open' pan-genome of African swine fever virus. Transbound. Emerg. Dis. 67, 1553–1562.

Wang, X., Wu, J., Wu, Y., Chen, H., Zhang, S., Li, J., Xin, T., Jia, H., Hou, S., Jiang, Y., 2018. Inhibition of cGAS-STING-TBK1 signaling pathway by DP96R of ASFV China 2018/1. Biochem. Biophys. Res. Commun. 506, 437–443.

Wang, Y., Kang, W., Yang, W., Zhang, J., Zheng, H., 2021. Structure of african swine fever virus and associated molecular mechanisms underlying infection and immunosuppression: a review. Front. Immunol. 12, 715582.

Yang, K., Huang, Q., Wang, R., Zeng, Y., Cheng, M., Xue, Y., Shi, C., Ye, L., Yang, W., Jiang, Y., Wang, J., Huang, H., Cao, X., Yang, G., Wang, C., 2021. African swine fever virus MGF505-11R inhibits type I interferon production by negatively regulating the cGAS-STING-mediated signaling pathway. Vet. Microbiol. 263, 109265.

Yang, K., Xue, Y., Niu, H., Shi, C., Cheng, M., Wang, J., Zou, B., Wang, J., Niu, T., Bao, M., Yang, W., Zhao, D., Jiang, Y., Yang, G., Zeng, Y., Cao, X., Wang, C., 2022. African swine fever virus MGF360-11L negatively regulates cGAS-STING-mediated inhibition of type I interferon production. Vet. Res. 53, 7.

Zhang, K., Yang, B., Shen, C., Zhang, T., Hao, Y., Zhang, D., Liu, H., Shi, X., Li, G., Yang, J., Li, D., Zhu, Z., Tian, H., Yang, F., Ru, Y., Cao, W.J., Guo, J., He, J., Zheng, H., Liu, X., 2022. MGF360-9L is a major virulence factor Associated with the african swine fever virus by antagonizing the JAK/STAT signaling pathway. mBio 13, e0233021.

Zhao, D., Liu, R., Zhang, X., Li, F., Wang, J., Zhang, J., Liu, X., Wang, L., Zhang, J., Wu, X., Guan, Y., Chen, W., Wang, X., He, X., Bu, Z., 2019. Replication and virulence in pigs

of the first African swine fever virus isolated in China. Emerg. Microb. Infect. 8, 438–447.
Zhu, J.J., Ramanathan, P., Bishop, E.A., O'donnell, V., Gladue, D.P., Borca, M.V., 2019. Mechanisms of African swine fever virus pathogenesis and immune evasion inferred from gene expression changes in infected swine macrophages. PLoS One 14, e0223955.
Zsak, L., Lu, Z., Burrage, T.G., Neilan, J.G., Kutish, G.F., Moore, D.M., Rock, D.L., 2001. African swine fever virus multigene family 360 and 530 genes are novel macrophage host range determinants. J. Virol. 75, 3066–3076.
Zsak, L., Neilan, J.G., 2002. Regulation of apoptosis in African swine fever virus-infected macrophages. Sci. World J. 2, 1186–1195.